# Comparisons of passive microwave remote sensing sea ice concentrations with ship-based visual observations during the CHINARE Arctic summer cruises of 2010-2018

Xiu, Yuanren

2020-09

Xiu , Y , Li , Z , Lei , R , Wang , Q , Lu , P & Lepparanta , M 2020 , ' Comparisons of passive microwave remote sensing sea ice concentrations with ship-based visual observations during the CHINARE Arctic summer cruises of 2010-2018 ' , Acta Oceanologica Sinica , vol. 39 , no. 9 , pp. 38-49 . https://doi.org/10.1007/s13131-020-1646-5

http://hdl.handle.net/10138/335159
https://doi.org/10.1007/s13131-020-1646-5

acceptedVersion

# Comparisons of passive microwave remote sensing sea ice concentrations with ship-based observations in the summer Arctic

**Abstract**

We compare the sea ice concentrations (SIC) of six long time series passive microwave (PM) products with that of 3890 ship-based observations (OBS) collected during seven Chinese National Arctic Research Expeditions. OBS SIC is collected according to the Antarctic Sea Ice Processes and Climate (ASPeCt) protocol. Six kinds of PM SIC are derived from the NASA-Team (NT), Bootstrap (BT) and Climate Data Record (CDR) algorithm based on SSM/I-SSMIS sensors, and the BT, enhanced NASA-Team (NT2) and ARTIST Sea Ice (ASI) algorithm based on AMSR-E/AMSR-2 sensors. Before comparing, in order to minimize the difference in spatial and temporal resolution between PM SIC and OBS SIC, we average the two kinds of data firstly. We compare the correlation coefficients (CC), average deviations and root mean square deviations (RMSD) between PM SIC and OBS SIC. Our results show that for the overall comparisons, CC values range from 0.84 (AMSR-E/AMSR-2 NT2) to 0.90 (SSM/I-SSMIS NT and AMSR-E/AMSR-2 BT). Average deviations range from −7.16% (SSM/I-SSMIS NT) to 8.48% (AMSR-E/AMSR-2 NT2). RMSD values range from 15.51% (SSM/I-SSMIS NT) to 22.27% (AMSR-E/AMSR-2 NT2). We also compare PM SIC with OBS SIC in different voyages and under different ice conditions in this paper. All in all, there are better agreements between OBS SIC and SSM/I-SSMIS NT, AMSR-E/AMSR-2 BT and ASI SIC in the summer Arctic.

**Key words:** Arctic, summer, sea ice concentration, passive microwave remote sensing, ship-based observations, comparison

## 1 Introduction

As an intuitive and sensitive indicator of global climate change, Arctic sea ice plays an important role in the global climate system (Vihma, 2014; Overland et al., 2015; Sui et al., 2017). Under the background of global warming, the Arctic has warmed twice as fast as the global average. This phenomenon is widely known as the "Arctic Amplification Effect" (Pithan and Mauritsen, 2014; Cohen et al., 2014). The rapid warming of the Arctic has led to the drastic melting of Arctic sea ice. Since October 1978, when there were continuous satellite observations, a large number of related studies have shown that the extent, area, concentration, thickness and the proportion of multi-year ice of Arctic sea ice have decreased significantly (Comiso, 2002; Comiso, 2012; Lei et al., 2015; Chen and Zhao, 2017; Serreze and Meier, 2019; Wang et al., 2019). The rapid melting of Arctic sea ice undoubtedly brings unprecedented convenience to navigation, resource development and *in situ* scientific investigation in the Arctic. Therefore, it is of great significance to grasp the temporal and spatial variation of Arctic sea ice as accurately as possible for the study of global climate change, the forecast of Arctic sea ice conditions, the design and construction of Arctic ocean engineering and its safe operation.

As an important parameter of many ocean and atmospheric circulation models, sea ice concentrations (SIC) is of great significance to the study of global climate change. Because the Arctic sea ice cover area is vast, the geographical location is remote, and the field observation is

difficult, remote sensing observation provides an irreplaceable data source for grasping the Arctic sea ice conditions (McIntire and Simpson, 2002). At present, remote sensing sensors for SIC observation mainly include visible-infrared sensors, passive microwave (PM) remote sensing sensors, active microwave (AM) remote sensing sensors and so on. Among them, visible-infrared sensors (such as the moderate-resolution imaging spectroradiometer, MODIS) have the advantage of high spatial resolution, but the disadvantage is that it is difficult to observe effectively under the conditions of cloud, fog and polar night (Liu et al., 2004). The advantage of PM sensors is that they have excellent long-wave penetration ability and can solve the problems of distinguishing sea ice from cloud and continuous observation of sea ice under polar night conditions, but the disadvantage is their low spatial resolution. AM sensors (such as the Synthetic Aperture Radar, SAR) combine the advantages of visible-infrared sensors and PM sensors. They can observe sea ice with high spatial resolution all day without the influence of weather and polar night. However, their cost is too high to use their data to establish global long-term sea ice time series climatic data sets. Given the above, PM remote sensing has become the preferred method for long-term continuous acquisition of large-scale polar sea ice horizontal distribution data. PM remote sensing obtains SIC by inputting the acquired brightness temperatures (Tb) data into the retrieval algorithms. Therefore, even if the same PM sensor is used, because different algorithms combine Tb data of different frequencies and polarization components, the final results of SIC retrievals are quite different. Many scholars have evaluated the performances of the PM algorithms by comparing the differences between the sea ice area, extent and concentration derived from different algorithms (Comiso et al. 1997; Ivanova et al., 2014; Hao and Su, 2015).

Only comparing different SIC retrieval algorithms is not enough to determine the reliability and validity of SIC retrieved by them. The most direct and effective way to evaluate the merits and demerits of SIC retrieval algorithm is to validate it by using field SIC data. The commonly used method is to regard SIC data obtained by means of ship-based observations (OBS), helicopter or unmanned aerial vehicle aerial photography (AP) in ice zones as ground truth value, and compare it with SIC retrieved by different sensors and algorithms (Worby and Comiso, 2004; Knuth and Ackley, 2006). Ozsoy-Cicek et al. (2009) found that compared with AMSR-E product, the National Ice Center (NIC) ice charts obtained from high resolution satellite images have better consistency with OBS data and AMSR-E product tends to underestimate ice conditions due to its low resolution during Antarctic summer. Ozsoy-Cicek et al. (2011) reported that the correlation between OBS data and PM data in the marginal ice zones (MIZ) of West Antarctica and over nearly the entire sea-ice zones of East Antarctica is less than that in 90°W region, and the extent of Antarctic sea ice estimated by AMSR-E data is 1-2×$10^6$ $km^2$ less than that estimated by NIC data. Beitsch et al. (2015) compared more than 21600 OBS SIC Around Antarctica with 7 kinds of PM SIC retrieved by five algorithms based on SSM/I-SSMIS and AMSR-E. Their results show that the Bootstrap (BT) algorithm is the best choice in both the SSM/I-SSMIS comparison and the AMSR-E comparison. Shi et al. (2015) used CHINARE-2012 helicopter AP and SAR images to evaluate the PM SIC based on the "HY-2" scanning radiometer in Arctic. Their results show that the SIC of "HY-2" products in the central Arctic Ocean is 16% higher than that of AP, and its root-mean-square with SAR is between 8.57% to 12.34%. By comparing the SIC extracted from ship-based monitoring images with SSMIS NT and AMSR-2 SICCI SIC data, Wang et al. (2018) reported that the SIC of SSMIS and AMSR-2 were 9.5% and 9.9% higher than the OBS SIC respectively, and the overestimations of SSMIS and AMSR-2 SIC increased to 12% and 16.4% respectively in areas the OBS SIC is less

than 15% , while the underestimations of SSMIS and AMSR-2 SIC are 4.4% and 8.9% in areas the OBS SIC is greater than 75%.

Although the PM SIC algorithm has been systematically evaluated in Antarctica by using a large number of OBS data, to our knowledge, the evaluation of PM SIC algorithm in Arctic is mostly based on the OBS data during a single expedition or voyage at present, which has many temporal and spatial limitations and can't exclude the deviations caused by some accidental factors. In this paper, we use a large number of OBS SIC data collected during the seven Chinese Arctic scientific expeditions (CHINARE) to compare with the six long time series PM SIC products used commonly. In the Section 2, we introduce the PM sensors, SIC retrieval algorithms and products, OBS data, data preprocessing and comparison methods firstly. In the Section 3, we show and describe the results of the comparisons. In the Section 4, we analyze and discuss the cause of error in SIC retrievals. The Section 5 is the conclusion of this paper.

## 2 Data and methods

### 2.1 *PM sensors*

PM sensors are important sensors for acquiring SIC at global or hemispheric scale. Their continuous observation ability lays a foundation for SIC monitoring and analysis of long time series. At present, the main PM sensors for SIC retrievals are SSM/I, SSMIS, AMSR-E, AMSR-2 and so on.

Since 1987, SSM/I sensors had been launched onboard the Defense Meteorological Satellite Program (DMSP) satellites. These satellites orbit the Earth in a near-polar solar synchronous orbit with an orbit period of about 102 minutes and a total of 14.1 r/day (Hollinger et al., 1990). Within one day, the polar region can be almost completely covered. SSM/I is a multi-channel PM sensor, which scans about 1400 km wide ground scenes (Hollinger et al., 1990) at a constant angle of incidence of 53.1 degrees (Kern and Heygster, 2001). In 2003, SSMIS replaced SSM/I for installation on DMSP F-16 and its successor satellites. SSMIS augments the imaging channel of SSM/I by several atmospheric sounding channels, but still has the ability of SSM/I to record Tb, among which the 19 GHz, 22 GHz, 37 GHz and 85 GHz imaging channels are associated with SIC retrievals (Beitsch et al., 2015). 85 GHz channel as the high frequency channel can provide higher spatial resolution. Using SSM/I and SSMIS as well as earlier SSMR, SIC products with spatial resolution of 25 km × 25 km and 12.5 km × 12.5 km from 1978 to now can be used for global climate change analysis.

AMSR-E was launched onboard the Aqua satellite on May 2, 2002 and ceased operation on December 4, 2011. The time coverage of its data ranges from 18 June 2002 to 4 October 2011. Like DMSP satellites, Aqua also orbits the Earth in near-polar solar synchronous orbit. Compared with SSM/I, AMSR-E has the main advantage of the high spatial resolution. The spatial resolution of AMSR-E based on 89GHz is 10 times higher than that of SSM/I based on 37 and 19 GHz channels (Spreen et al., 2008). AMSR-2, as the successor to AMSR-E, was launched onboard the Global Change Observation Mission for Water-1 (GCOM-W1) satellite by the Japan Aerospace Exploration Agency (JAXA) on May 1, 2012. The main mission of AMSR-2 is to detect the earth's water and energy cycle. The scanning angle of incidence is 55 degrees and provide a 1450-km swath width at the Earth's surface (Beitsch et al., 2014). Compared with AMSR-E, AMSR-2 adds two channels of 7.3GHz, which can be used to relieve radio frequency interference (RFI). The size of

its main reflector has increased to 2.0m, which leads to smaller footprints and improves the spatial resolution for different frequencies (Beitsch et al., 2014). At present, SIC products with spatial resolution up to 3.125 km × 3.125 km can be obtained by using AMSR-E and AMSR-2.

Because the PM SIC data sets used in this paper uses multiple sensors over time, they are SSM/I-SSMIS sensors and AMSR-E/AMSR-2 sensors, in order to ensure the consistency of data, each product calibrates the algorithms of different sensors, so the source of Tb data is not important. For SSM/I and SSMIS data sets, the tie points are adjusted by regression analysis of two brightness temperatures during the overlap of the two sensors working time to make the derived sea ice fields as consistent as possible (Comiso and Nishio, 2008). For AMSR-E and AMSR-2 data sets, the main method is to convert AMSR-2 Tb to equivalent AMSR-E Tb after regression analysis of AMSR-2 Tb and AMSR-E Tb, so that two sensors using the same algorithm will not have a significant impact on the SIC retrievals (Meier and Ivanoff, 2017). From here on, when we refer to SSMIS, we refer to the combined SIC database of SSM/I and SSMIS. When we refer to AMSR, we refer to the combined SIC database of AMSR-E and AMSR-2.

### 2.2 *SIC retrieval algorithms and products*

The PM SIC data used in this paper are derived from six long time series SIC products which are commonly used and still being updated. They are corresponding products of NT, BT and Climate Data Record (CDR) algorithm based on SSMIS sensors and those of BT, enhanced NASA-Team (NT2) and ARTIST Sea Ice (ASI) based on AMSR sensors.

The basic principle of the NT algorithm is to use the PM sensors' 19 GHz vertical and horizontal, 37 GHz vertical polarization Tb to calculate Polarization ratios (PR) and gradient ratios (GR) to identify the sea water, first-year ice and multi-year ice, and so as to retrieve SIC (Smith, 1996). The SSMIS-NT SIC product used in this paper is provided by the National Snow and Ice Data Center (NSIDC) with a grid resolution of 25 km × 25 km.

The basic principle of BT algorithm is to identify sea water and sea ice by using the differences of polarization Tb between 37GHz vertical and horizontal channels and between 37GHz vertical and 19Hz horizontal channels, and so as to retrieve SIC (Smith, 1996). The SSMIS-BT SIC product used in this paper is provided by NSIDC with a grid resolution of 25 km × 25 km. The AMSR-BT SIC product used in this paper is provided by University of Bremen (UB) with a grid resolution of 6.25 km × 6.25 km.

CDR algorithm comes from the combination of NT algorithm and BT algorithm for SIC retrievals (Peng et al., 2013). CDR algorithm tries to utilize the advantages of NT algorithm and BT algorithm to generate SIC field more precise than these two algorithms. The SSMIS-CDR SIC product used in this paper is provided by NSIDC with a grid resolution of 25 km × 25 km.

NT2 algorithm is an improved algorithm designed to solve some problems existing in the SIC retrievals of NT algorithm. NT2 algorithm calculates PR and GR in the same way as NT algorithm. In order to avoid the influence of snow cover on ice type identification, $PR_R$ is calculated and the polarization Tb of high frequency (85GHz for SSMIS and 89GHz for AMSR) vertical and horizontal channel is used to calculate ΔGR to estimate the surface effect (Markus and Cavalieri, 2000). The AMSR-NT2 SIC product used in this paper is provided by NSIDC with a grid resolution of 12.5 km × 12.5 km.

ASI algorithm was developed from the Arctic Radiation and Turbulence Interaction Study (ARTSIST) in 1998. The ASI algorithm only uses the difference between the polarization Tb of

89GHz horizontal and vertical channels to retrieve SIC, and uses low frequency Tb as weather filter to filter out the misjudgements of SIC caused by atmospheric water vapor in some MIZ and the ice-free area (Spreen et al., 2008). Compared with other high-frequency algorithms, the ASI algorithm can achieve similar results with the SIC algorithm using other extra channels without additional data sources. (Kern et al., 2003). However, the precondition for ASI algorithm to determine the tie point is to make the result of SIC retrievals closest to the that of BT algorithm (Spreen et al., 2008). As a result, the result of SIC retrievals of ASI algorithm depend on the retrieval accuracy of BT algorithm. The AMSR-ASI SIC product used in this paper is provided by UB, and the grid resolution is 3.125 km × 3.125 km.

### 2.3 *ASPeCt OBS data*

The ASPeCt OBS data used in this paper are from the CHINARE-2003, CHINARE-2008, CHINARE-2010, CHINARE-2012, CHINARE-2014, CHINARE-2016 and CHINARE-2018. The quantity of these data is 3890. The tracks of these voyages are shown in Fig. 1.

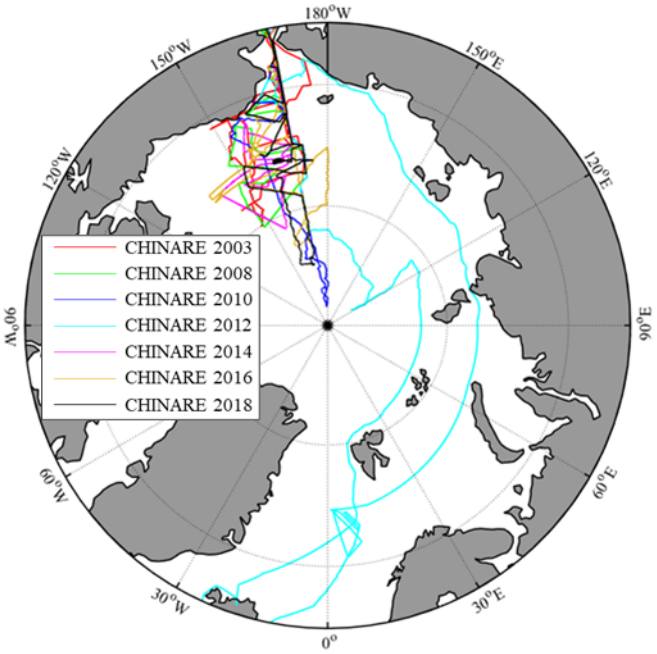


Fig.1. The sketch map of Chinese national Arctic research expedition routes used in this paper.

When the R/V *Xuelong* icebreaker was sailing in the ice zones, according to the ASPeCt OBS standard, namely, the ASPeCt protocol (Worby et al., 1999), sea ice was divided into three types to record their concentration, growth stage, size and thickness, as well as the snow layer thickness on the ice surface and the coverage rate of melt ponds and ice ridges. The method of SIC artificial observation is that the observer stands on the bridge and estimates the proportion of sea ice area within the sight range of about 1 km with his eyes to determine the SIC (in tenths) of the current location according to the definition of SIC in WMO (1970), as shown in Fig. 2. When the speed is less than 6 knots, the ice condition is observed and recorded every hour; when the speed is greater than 6 knots, the ice condition is observed and recorded every half hour, the duration of a single observation is 5-10 minutes. When the expedition carries out short-term (within one day) or long-term (several days or more) observation in the ice station, the R/V *Xuelong* icebreaker will stop

sailing and the artificial observation of sea ice will also be suspended.

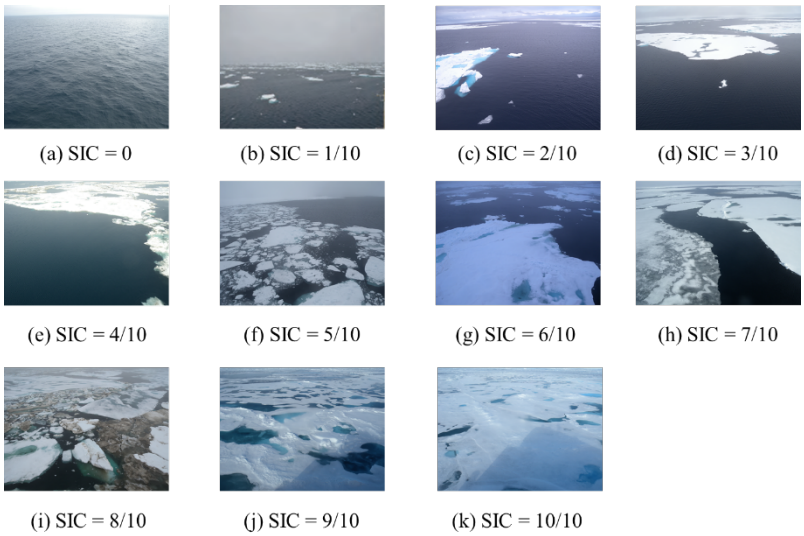


Fig.2. Examples of different SIC during navigation.

Since OBS SIC is evaluated in tenths, rounding errors can be as high as 5% in theory (Worby and Comiso, 2004). In addition, due to the subjectivity of the observer, it is difficult to quantify the differences in the evaluation of OBS SIC among different observers. However, experiments have shown that when different observers observe at the same time, the overall SIC difference assessed is rarely more than 10% (Worby and Comiso, 2004). Weissling et al. (2009) proposed that the average deviation of SIC observations of ASPeCt is less than 10%.

### 2.4 *Data preprocessing and comparison methods*

The OBS SIC represents the average SIC within an elliptical range of about 1 km in the short half-axis observed for 5-10 minutes from a certain time, which is given in tenths. The PM SIC gives the average SIC of each grid cell in a percentage form in one day. The minimum grid size of PM SIC products used in this paper is 3.125 km × 3.125 km, and the maximum is 25 km × 25 km. The temporal and spatial scale of OBS data is much smaller than that of PM data, so it is more changeable. There are 3890 OBS data used in this paper, and the quantity of them is quite large. For the above reasons, there may be some problems in comparing the two kinds of data directly.

In order to minimize the impact of inconsistent spatial and temporal scales of the two kinds of data on the comparison, before comparing the data, this paper decides to average the OBS SIC and the PM SIC of the same day. Specifically, for each OBS SIC, find the PM SIC of the same date and the nearest grid in each SIC product. Then the average values of OBS SIC and PM SIC corresponding to each other in the same day are calculated and compared. This method is similar to the method used by Beitsch et al. (2015) to average the two data on the same day along the track. The R/V *Xuelong* icebreaker did not always sail at a uniform speed in the ice zones. When it encounters severe ice conditions, the speed of the R/V *Xuelong* icebreaker will slow down. For example, when encountering a large number of ice ridges, the R/V Xuelong icebreaker may even travel for only a few hundred meters in an hour. However, the maximum grid size of PM products used in this paper is up to 25km × 25km, so it is inevitable that multiple OBS SICs correspond to the same PM SIC (see Fig. 3). The method used in Beitsch et al. (2015) is similar to calculate the

arithmetic average of OBS SIC but calculate the weighted average for PM SIC as Shown in Eq. (1):

$$C_{PM} = \frac{C_1 + C_2 + C_3 + C_4 + C_5 + C_6}{6}, \quad (1)$$

As shown in Fig. 3, $C_{PM}$ is the average of PM SIC in one day and $C_i$ is the PM SIC in the corresponding grid.

As a result, the weight of the same PM SIC corresponding to multiple OBS SICs is reduced. The average method in this paper is to calculate the arithmetic average of PM SIC and that of OBS SIC as shown in Eq. (2):

$$C_{PM} = \frac{C_1 + C_2 + C_3 + 3C_4 + 2C_5 + C_6}{9}, \quad (2)$$

As shown in Fig. 3, $C_{PM}$ is the average of PM SIC in one day and $C_i$ is the PM SIC in the corresponding grid.

In this way, the statistical distribution characteristics between the original data are maintained to a greater extent.

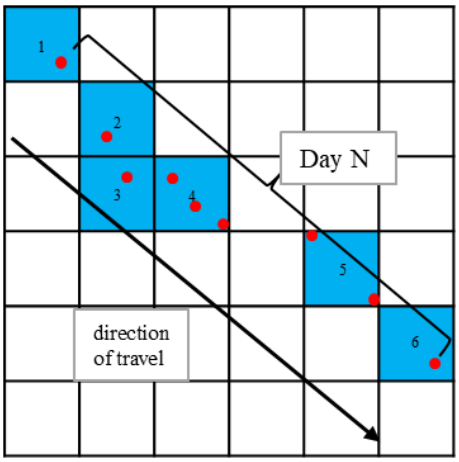


Fig.3. Schematic map of OBS SIC and PM SIC, the red dot represents the position of OBS SIC, and the blue square represents the PM SIC grid in which the red dot falls,the number in the grid is the number of the grid. See text for explanation.

After the preprocessing of the two kinds of data, we calculate the correlation coefficients (CC), average deviations and root mean square deviations (RMSD) between each PM SIC and OBS SIC as the basis for evaluating the retrieval accuracy of each product.

## 3 Results

### *3.1 Overall Comparisons between PM SIC and OBS SIC*

After the preprocessing of the two kinds of data, 174 groups of daily average SIC data were obtained. Comparing the daily average PM SIC with the daily average OBS SIC, the results are shown in Fig. 4 and Table 1.

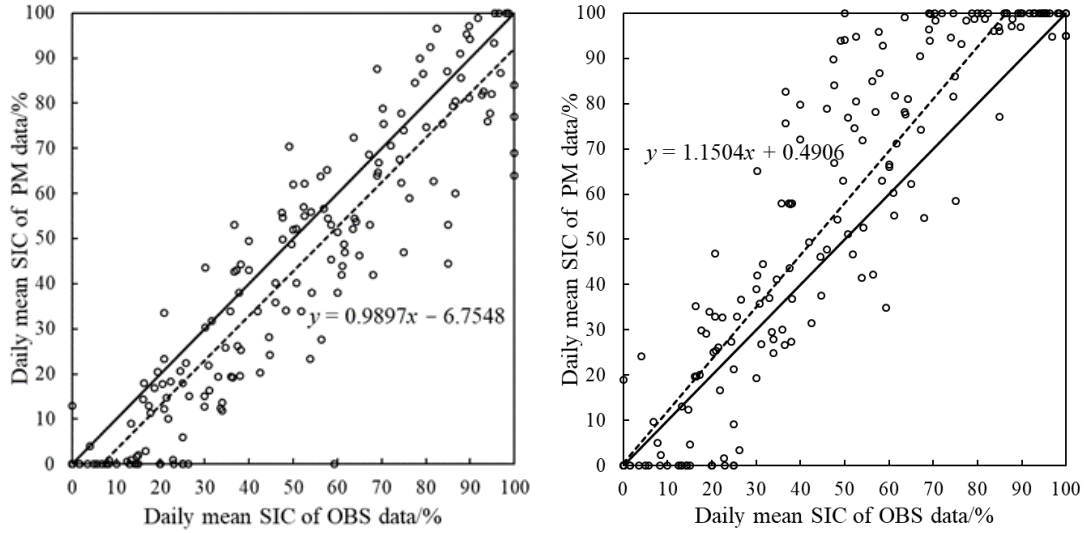


(a) SSMIS-NT




(b) SSMIS-BT

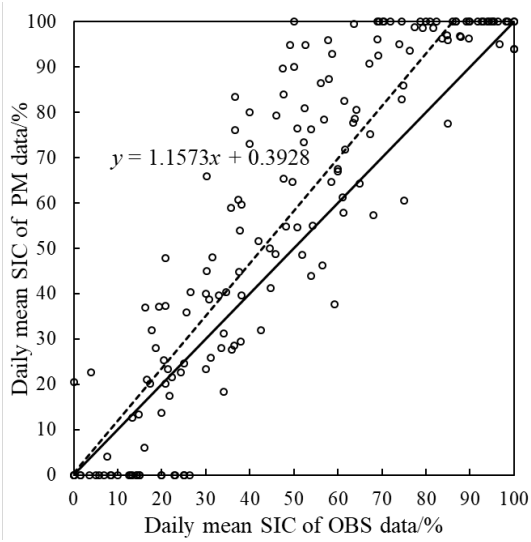


(c) SSMIS-CDR

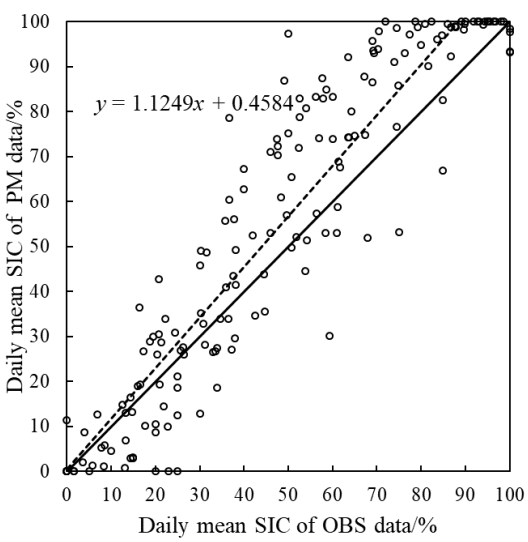


(d) AMSR-BT

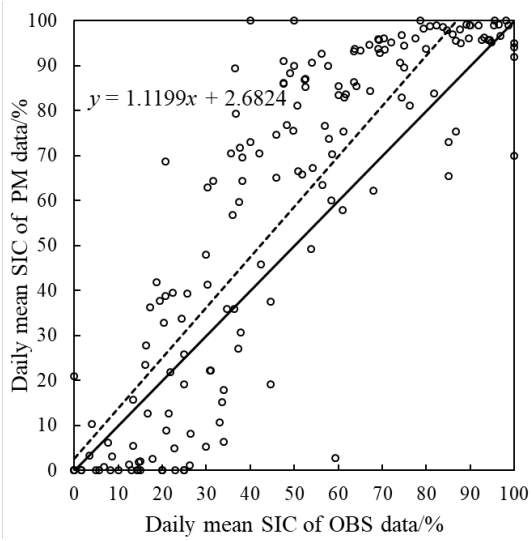


(e) AMSR-NT2

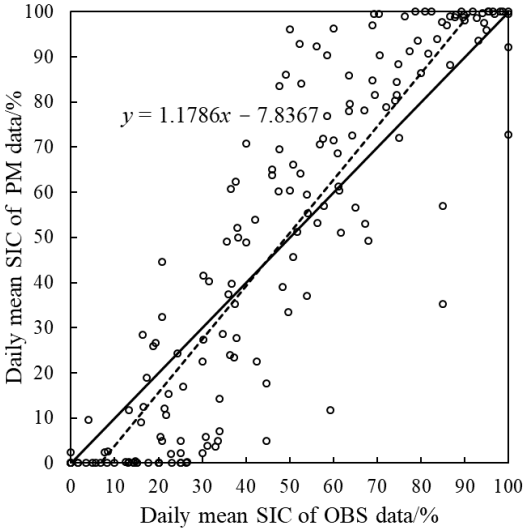


(f) AMSR-ASI

Fig.4. Comparison of daily mean SIC between OBS data and PM data (The solid line represents $y = x$, the dotted line represents linear fitting result, the equation is the linear regression equation of

the dotted line).

Table 1. Summary of statistical results of PM SIC comparing with OBS SIC

| | Correlation coefficient | Average deviation/% | RMSD/% |
|---|---|---|---|
| SSMIS-NT | 0.90 | −7.16±13.76 | 15.51 |
| SSMIS-BT | 0.88 | 7.82±18.02 | 19.64 |
| SSMIS-CDR | 0.88 | 8.06±18.18 | 19.88 |
| AMSR-BT | 0.90 | 6.57±15.38 | 16.73 |
| AMSR-NT2 | 0.84 | 8.48±20.59 | 22.27 |
| AMSR-ASI | 0.88 | 1.18±18.89 | 18.92 |

As can be seen from Fig. 4, SSMIS-NT tends to underestimate SIC in overall compared with OBS SIC. Sea ice is often not observed at low OBS SIC (0-15%). SSMIS-BT and SSMIS-CDR also tend to underestimate SIC or even fail to observe sea ice when OBS SIC < 15%. When OBS SIC > 30%, it tends to overestimate SIC. When OBS SIC > 70%, the whole observation range is usually judged to be completely covered by sea ice. AMSR-BT tends to underestimate SIC when OBS SIC < 15% and overestimate SIC when OBS SIC > 30%. When OBS SIC > 80%, the whole observation range is usually judged to be completely covered by sea ice. AMSR-NT2 tends to underestimate SIC when OBS SIC < 15% and overestimate SIC when OBS SIC > 30%. AMSR-ASI tends to underestimate SIC or even fail to observe sea ice when OBS SIC < 15%. It tends to overestimate SIC when OBS SIC > 40%. When OBS SIC > 80%, it tends to judge the whole observation area as completely covered by sea ice.

From Table 1, it can be seen that the CC between six kinds of PM SIC and OBS SIC are not significantly different. The CC values of SSMIS-NT and AMSR-BT are the largest, both of which are 0.90. The CC values of SSMIS-BT, SSMIS-CDR and AMSR-ASI are all 0.88. The CC value of AMSR-NT2 is the smallest, which is 0.84. The average deviation between SSMIS-NT SIC and OBS SIC is negative, which is −7.16%, indicating that SSMIS-NT underestimates SIC in overall compared. The absolute value of average deviation between AMSR-ASI SIC and OBS SIC is the smallest, which is only 1.18%. That value of AMSR-NT2 is the largest, which is 8.48%. Those values of AMSR-BT, SSMIS-BT and SSMIS-CDR are 6.57%, 7.82% and 8.06% respectively. The RMSD between SSMIS-NT SIC and OBS SIC is the smallest, which is 15.51%. That value of AMSR-NT2 is the smallest, which is 22.27%. Those values of AMSR-BT, AMSR-ASI, SSMIS-BT and SSMIS-CDR are 16.73%, 18.92%, 19.64% and 19.88%, respectively. Although the absolute value of average deviation between AMSR-ASI SIC and OBS SIC is the smallest, RMSD is larger, which indicates that the deviation between AMSR-ASI SIC and OBS SIC is sometimes positive and sometimes negative, and the positive and negative deviations offset each other when calculating average deviation.

From the above overall comparison results, the SIC retrieved by SSMIS-NT, AMSR-BT and AMSR-ASI are closer to that of OBS SIC.

### 3.2 *Comparisons between PM SIC and OBS SIC in different voyages*

Divide the data into different voyages for statistics, the quantities of OBS data of each voyage are 27, 24, 18, 23, 27, 26 and 29, respectively. The statistical results of the CC, average deviation and RMSD between PM SIC and OBS SIC for each voyage are shown in Fig. 5-7.

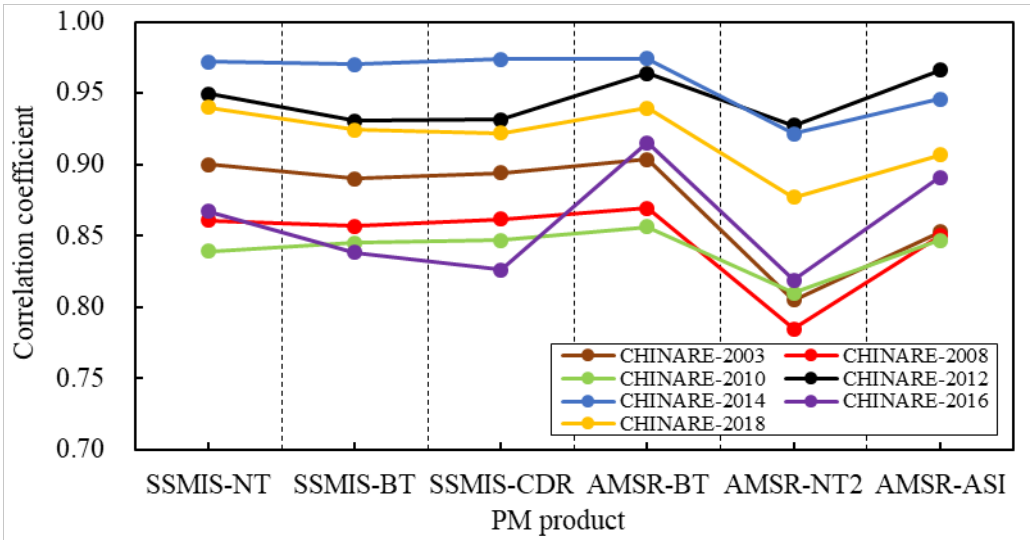


Fig.5. Statistical results of CC between PM SIC and OBS SIC in different voyages.

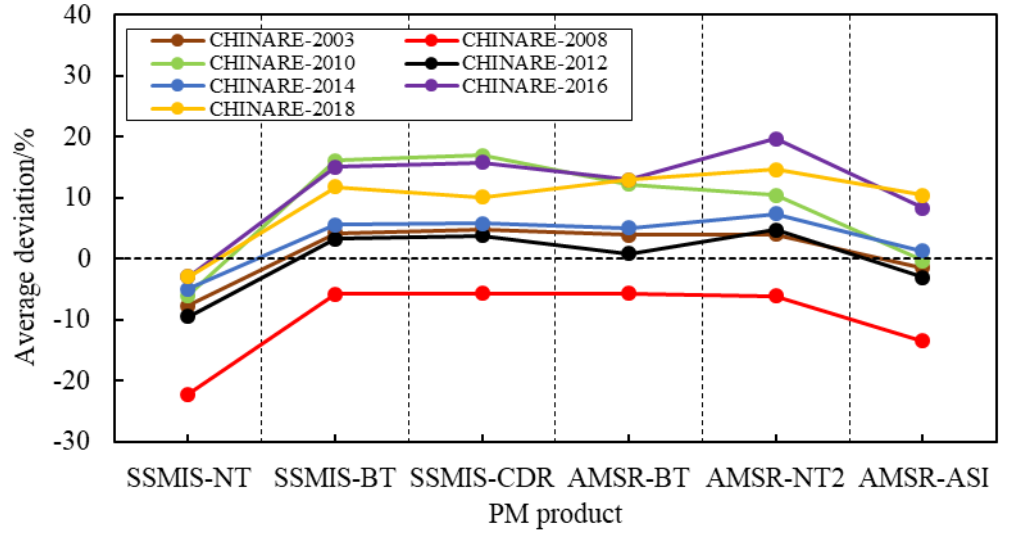


Fig.6. Statistical results of average deviation between PM SIC and OBS SIC in different voyages.

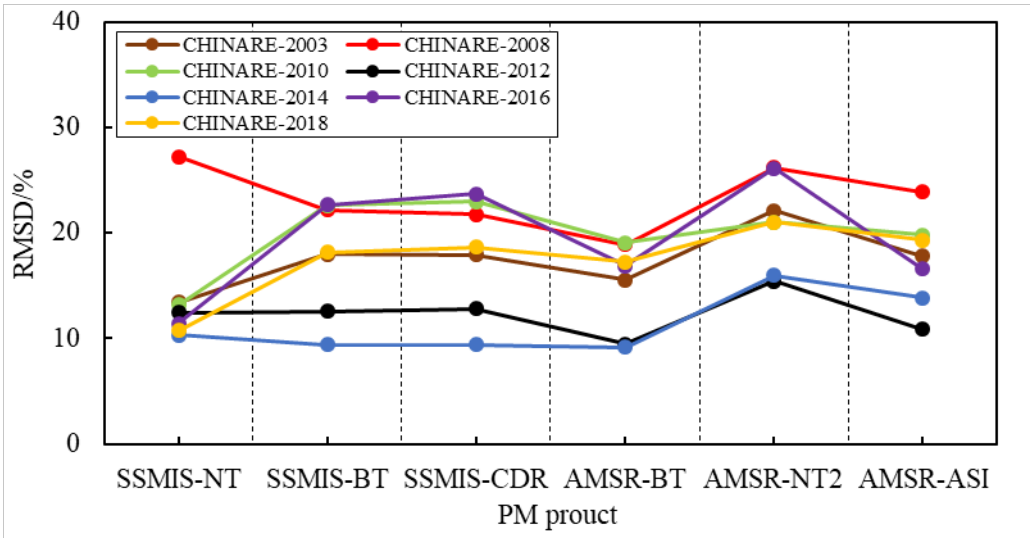


Fig.7. Statistical results of RMSD between PM SIC and OBS SIC in different voyages.

It can be seen from Fig. 5 that the CC values between PM SIC and OBS SIC vary in different voyages, but the relationship between the CC values of PM SIC and OBS SIC is basically the same in the same voyage. In almost all voyages, the CC values between AMSR-BT SIC and OBS SIC is the largest, while that between AMSR-NT2 SIC and OBS SIC is the smallest.

Figure 6 shows that the average deviation between SSMIS-NT SIC and OBS SIC is negative in all voyages, which indicates that SSMIS-NT products underestimate SIC in all voyages. Obviously, in different voyages, the average deviation between PM SIC and OBS SIC varies, but the relationship between the values of PM SIC and OBS SIC is basically the same in the same voyage. Among the six PM products, the absolute value of the average deviation between AMSR-ASI SIC and OBS SIC is smaller in most voyages.

As can be seen from Fig. 7, RMSD between PM SIC and OBS SIC also changes in different voyages, and the relationship between the values of PM SIC and OBS SIC is also basically the same in the same voyage. Except for very few voyages, the RMSD between AMSR-ASI SIC and OBS SIC is larger than that of SSMIS-NT and AMSR-BT, which indicates that the deviation between AMSR-ASI SIC and OBS SIC is sometimes positive and sometimes negative, and offsets each other when calculating the average deviation. In almost all voyages, the RMSD of AMSR-NT2 SIC and OBS SIC are the largest, so its retrieval accuracy is the worst.

### 3.3 *Comparisons between PM SIC and OBS SIC under different ice conditions corresponding to OBS data*

According to the WMO (1970) description of the relationship between SIC and ice conditions, and referring to the definition of the relationship between sea ice cover and ship navigation difficulty defined by Shibata et al. (2013), in this paper, SIC is divided into three types: 0-30%, 30-70% and 70-100%. They correspond to light ice condition (easy to navigate), medium ice condition (a little difficult to navigate) and heavy ice condition (very difficult to navigate) respectively. The quantities of OBS data corresponding to the three ice conditions are 56, 73 and 45, respectively. According to the three ice conditions corresponding to OBS data, the CC, average deviation and RMSD between six kinds of PM SIC and OBS SIC are calculated. The results are shown in Fig. 8-10.

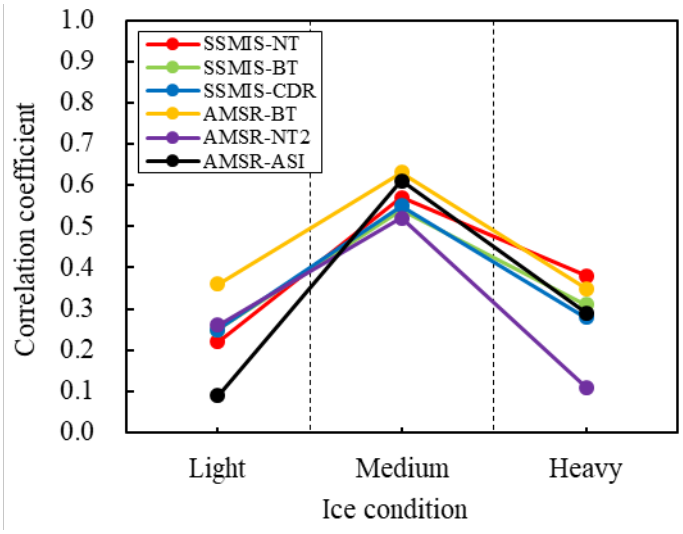


Fig.8. Statistical results of CC between PM SIC and OBS SIC under different ice conditions corresponding to OBS data.

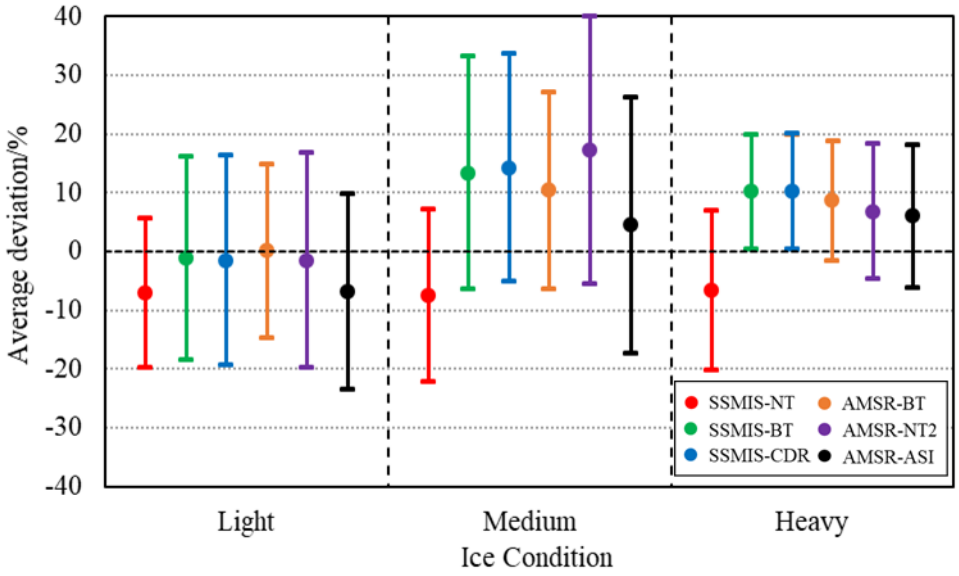


Fig.9. Statistical results of average deviation between PM SIC and OBS SIC under different ice conditions corresponding to OBS data.

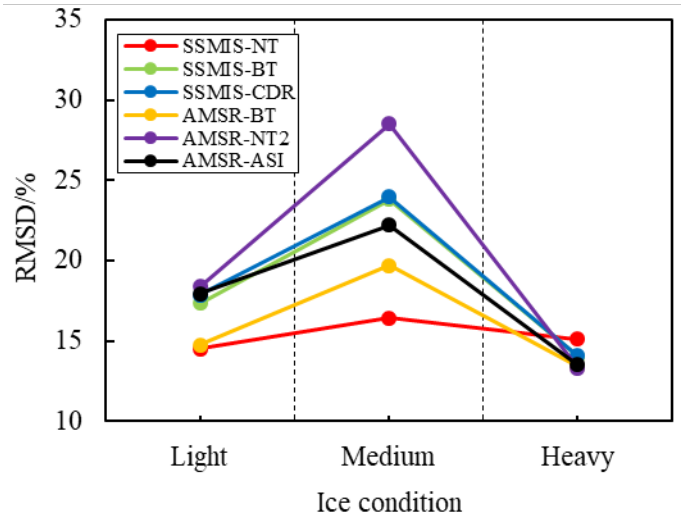


Fig.10. Statistical results of RMSD between PM SIC and OBS SIC under different ice conditions corresponding to OBS data.

From Fig. 8, we can see that the CC between PM SIC and OBS SIC are significantly reduced compared with the overall comparisons. The CC between PM SIC and OBS SIC are the greatest under the medium ice condition corresponding to OBS data, while those under the light ice condition and the heavy ice condition are very small. The CC between AMSR-BT and OBS SIC is almost the largest under all ice conditions correspond to OBS data.

Figure 9 shows that the average deviation between SSMIS-NT SIC and OBS SIC is negative under all ice conditions corresponding to OBS data, which are −7.07%, −7.55% and −6.64%, respectively, which indicates that SSMIS-NT product underestimate SIC under any ice condition corresponding to OBS data. The average deviations of SSMIS-BT, AMSR-NT2, SSMIS-CDR and AMSR-ASI are negative under the light ice condition corresponding to OBS data, which are −1.14%, −1.54%, −1.57% and −6.85%, respectively. At this time, only the average deviation of AMSR-BT

is positive and only 0.02%, which indicates that PM products tend to underestimate SIC when the actual ice condition is light. The average deviations between the other five kinds of PM SIC and OBS SIC were positive under the medium ice condition corresponding to OBS data, which are 13.29%,14.15%, 10.36%, 17.22% and 4.39%, respectively. Under the heavy ice condition corresponding to OBS data, the average deviations are 10.11%, 10.17%, 8.58%, 6.77% and 5.97%, respectively. It indicates that the other five kinds of PM products except SSMIS-NT tend to overestimate SIC when the concentration is high, and the average deviations are larger under the medium ice condition corresponding to OBS data than under the heavy ice condition.

It can be seen from Fig. 10 that RMSD between PM SIC and OBS SIC is the smallest under the heavy ice condition corresponding to OBS data, followed by light ice condition, and the largest under the medium ice condition corresponding to OBS data. Under all ice conditions corresponding to OBS data, the RMSD between SSMIS-NT SIC and OBS SIC are all close to 15%. The RMSD of SSMIS-BT and SSMIS-CDR are similar under all ice conditions corresponding to OBS data, and smaller than that of SSMIS-NT only under the heavy ice condition corresponding to OBS data. The RMSD of AMSR-BT SIC are small under all ice conditions correspond to OBS data, which are 14.78%, 19.72% and 13.40%, respectively. The RMSD of AMSR-NT2 and AMSR-ASI are similar under the light and heavy ice conditions corresponding to OBS data, which are 18.40% and 17.96%, 13.32% and 13.52%, respectively. Under the medium ice condition corresponding to OBS data, they are 28.51% and 22.21%. It can be seen that although the absolute of average deviations between PM SIC and OBS SIC are very small Under the light ice condition corresponding to OBS data, the RMSDs are larger than those under the heavy ice condition. According to Fig. 4, although we regard the SIC of 0 to 30% as light ice condition, PM products generally underestimate SIC when OBS SIC is 0 to 15%, while PM products generally overestimate SIC when OBS SIC is 15 to 30%, offsetting each other when calculating average deviations.

From the above Comparisons, under different ice conditions corresponding to OBS data, SSMIS-NT, AMSR-BT and AMSR-ASI data are closer to OBS data, and their SIC retrievals are more accurate.

## 4 Discussion

According to the comparisons between PM SIC and OBS SIC, it can be seen that the retrieval accuracy of SSMIS-NT, AMSR-BT and AMSR-ASI is better than that of SSMIS-BT, SSMIS-CDR and AMSR-NT2. The differences of sensors and algorithms used in various PM products determines the differences of SIC derived from them.

Compared with SSMIS sensors, the main advantage of AMSR sensors is that they improve the resolution of all scanning channels. The spatial resolution of ASI products based on 89GHz channel Tb has reached 3.125 km × 3.125 km, so more details can be obtained in small spatial scales when retrieving SIC. For example, the high resolution AMSR sensors can observe more precise ice edges, and reduce the uncertainty caused by surface parameters. Therefore, compared with SSMIS-NT product, the high resolution of AMSR-BT product and AMSR-ASI product can provide more surface information. This has great advantages for navigation and small-scale ocean engineering applications.

The essence of the differences of SIC obtained by PM algorithms is that the methods of retrieving SIC from Tb data provided by sensors are different. It is mainly caused by the different selections and uses of channels, weather filters and tie points and the different sensitivities of the algorithms

to the physical temperature changes in the emitting layer (Comiso et al., 1997). NT and NT2 algorithms mainly use Tb ratios for SIC retrievals, so they can offset any changes in the physical temperature of the emitting layer. BT and ASI algorithm use the difference between the two Tb for SIC retrievals, so the retrieval effect will be affected by the physical temperature changes from the emitting layer.

Andersen et al. (2007) pointed out that the stratification of ice and snow on the surface and the existence of thin ice have a great influence on the horizontal polarization channel, especially when the thickness of thin sea ice is less than 20 cm, the microwave emissivities are usually low, which leads to the increase of PR value and the underestimation of SIC. Generally speaking, the higher the channel frequency is, the higher the spatial resolution of the retrieving SIC is. However, the wavelength of high frequency channel is shorter, so its penetration depth is shallower, which is more sensitive to the impact of snow on the sea ice surface, leading to the misjudgement of SIC. High frequency channels are more susceptible to atmospheric water vapor interference. When the water content in the atmosphere is high in thin ice zones, water vapor will be misjudged as sea ice, thus overestimating SIC (Spreen et al., 2008). In order to reduce the influence of atmospheric state on SIC retrievals, each algorithm calibrates the atmosphere or uses weather filters to filter out the water vapor and other components misjudged as sea ice outside the MIZ (Spreen et al., 2008). However, doing so cuts off low SIC values, and so, leads to the phenomenon that all kinds of PM products in Fig. 4 tend to underestimate SIC or even fail to observe sea ice when the OBS SIC < 15%.

Tie points are points with typical radiation signals for open water and sea ice. Usually, the most sensitive point with high signal-to-noise ratio is chosen as the tie point in the algorithm (Beitsch et al., 2015). The emissivity of sea ice varies greatly with ice age, thickness and surface roughness. Because of the differences of region, season and climate, the state parameters of sea ice vary greatly, which leads to the continuous change of the sea ice emissivity in different states. Using only fixed tie points will inevitably increase the uncertainty of the retrieval algorithm, thus reducing the reliability of the SIC retrievals. The use of dynamic tie points has become a trend of future algorithms. Arctic sea ice can be divided into first-year ice and multi-year ice. While the Southern Ocean has almost no multi-year ice. Sea ice in the Antarctic can only distinguish sea ice types according to different snow cover states. Although much work has been done to compare the OBS data in the Southern Ocean with remote sensing products, the results of the comparisons in the Southern Ocean can not be copied to the Arctic Ocean because of the great differences in sea ice state between the two oceans. However, the data in the Arctic are relatively scarce, so on the basis of accumulating a large amount of data from several Chinese National Arctic Research Expeditions, it is very necessary to compare the OBS data with remote sensing products in this paper. The results obtained above in this paper are also different from those of the Antarctic (Beitsch et al., 2015).

There is also a tendency for R/V *Xuelong* icebreaker to sail in thin ice or ice-free zones on the route when it sails in the ice zones. Therefore, we can not rule out that the OBS SIC will be somewhat low. Accordingly, as mentioned above, PM data also tend to underestimate SIC in thin ice zones, which reduces the impact of underestimating SIC theoretically by OBS data on comparative works. In Fig. 6, we find that the average deviations between all kinds of PM SIC and OBS SIC is negative during CHINARE-2008, while the average deviations between all kinds of PM SIC and OBS SIC is significantly larger during CHINARE-2016. This may be because the participants in each Arctic expedition are different, and OBS SIC inevitably has subjective errors from observers. However, the trends of the deviations between PM SIC and OBS SIC in different

voyages are basically consistent. In addition, this paper uses a large number of data from seven Chinese National Arctic Research Expeditions, which will cancel out the subjective errors of previous observers by averaging each other in the overall statistics. Therefore, we believe that our statistical results are credible. Next, we compare the statistical results of helicopter aerial photography (AP) data collected during the CHINARE-2010 with those of OBS data.

The helicopter AP work was mainly carried out when the R/V *Xuelong* icebreaker stopped and the short-term and long-term ice station observation was carried out. Canon G9 digital camera and GPS are mounted on the helicopter platform to take sea ice images along the way and record the GPS position of the images at the same time. Six sorties were flown in 2010 and 5619 images were obtained. The pixels of sea water, pure sea ice and melt ponds are distinguished by threshold segmentation. Then the SIC in the field of view of the image can be obtained by dividing the sum of the pixels of pure sea ice and melt ponds by the total number of pixels of the image. Because the helicopter route is not affected by the surface morphology, and the SIC is acquired from the vertical angle of view, the distortion error of the field of view is small, so the SIC acquired by aerial photography should be more accurate than OBS SIC. The helicopter AP SIC is also compared with the corresponding PM SIC after the same average treatment as OBS SIC. Average deviations and RMSD between OBS SIC and PM SIC and those between AP SIC and PM SIC during CHINARE-2010 are shown in Table 2. Table 2 shows that the statistical results of OBS data and AP data are in good agreement, which further confirms the reliability of our comparative work using OBS data.

Table 2. The Comparison between Statistical results of average deviation and RMSD between PM SIC and OBS SIC and those between PM SIC and AP SIC during CHINARE-2010

| | Average deviation/% | | RMSD/% | |
|---|---|---|---|---|
| | OBS | AP | OBS | AP |
| SSMIS-NT | −6.01±11.75 | −6.88±13.81 | 13.19 | 15.42 |
| SSMIS-BT | 16.08±15.89 | 19.60±15.49 | 22.61 | 24.98 |
| SSMIS-CDR | 16.93±15.47 | 20.27±14.86 | 22.93 | 25.13 |
| AMSR-BT | 12.27±14.63 | 14.28±13.26 | 19.09 | 19.49 |
| AMSR-NT2 | 10.41±18.26 | 13.17±18.30 | 21.02 | 22.54 |
| AMSR-ASI | −0.33±19.38 | 9.97±19.57 | 19.80 | 21.97 |

As can be seen from Fig. 1, except for CHINARE-2012, the tracks of the other six voyages are all in the Chukchi Sea, the Beaufort Sea and the central Arctic sea north of them. It is helpful to understand the advantages or limitations of different algorithms by distinguishing different regions in theory. However, we do not distinguish different regions, but consider the whole Arctic sea ice as a large-scale system to consider its overall long-term development status. The comparison based on this has enough representativeness and reliability, and it is difficult to estimate, understand and describe the more uncertainties introduced by the division of sub-regions.

All the voyages of the Chinese National Arctic Research Expeditions mentioned in this paper are in the summer Arctic. Generally speaking, the states of the sea ice in summer are more complicated than those in winter. In summer, due to the intense melting of sea ice, the existence of wet snow, melt ponds and the mixture of thin ice and water, the retrievals of sea ice properties becomes more complex (Ivanova et al., 2014), which leads to the decrease of retrieval reliability. Wang et al. (2018) pointed out that the inaccurate distinction between melt ponds and open waters was the main reason

why SSMIS-NT underestimated SIC in the summer Arctic. As a surface effect, the further development of melting state will lead to a larger area of open water in the regions, increase the influence of water vapor in the atmosphere, and then increase the uncertainty of SIC retrievals. Therefore, the comparison of summer SIC in this paper is actually to compare the performance of each algorithm in the most disadvantageous season, that is, the upper limit of the retrieval error of each algorithm in a year, which is helpful for us to understand the limitations of each PM SIC algorithm better, so as to provide some data references for improving the PM SIC algorithms.

In the future, we will make more systematic and detailed comparisons and evaluations of PM SIC products in the Arctic on the basis of collecting *in situ* observations in various regions and seasons in the Arctic.

## 5 Conclusions

We use OBS SIC data from seven Chinese National Arctic Research Expeditions to compare with six commonly used PM SIC products with long time series. OBS SIC is collected according to ASPeCt protocol, and PM products are based on SSMIS sensors and AMSR sensors. We compare the daily average OBS SIC with the nearest PM SIC of the same day after the same average processing. By calculating the correlation coefficients, average deviations and RMSDs between each PM SIC and OBS SIC, we can evaluate the retrieval accuracy of each product.

Our results show that in SSMIS PM products, although SSMIS-NT tend to underestimate SIC, the correlation coefficient between SSMIS-NT SIC and OBS SIC are larger than that of the other two kinds of SSMIS products. The absolute value of average deviation and RMSD between SSMIS-NT SIC and OBS SIC are smaller than those of the other two SSMIS products. Therefore, SSMIS-NT is the product with the highest retrieval accuracy in SSMIS products. Although SSMIS-BT product tends to underestimate SIC in the Southern Ocean (Beitsch et al., 2015), our results show that SSMIS-BT product overestimates SIC in the Arctic. SSMIS-CDR, which takes the larger values between SSMIS-NT and SSMIS-BT SIC retrievals as its own value, also overestimates SIC in the Arctic, which is less accurate than SSMIS-BT in theory. Among PM products of AMSR sensors, the correlation coefficient between AMSR-BT SIC and OBS SIC is the largest, the average deviation between AMSR-ASI SIC and OBS SIC is the smallest, the RMSD between AMSR-BT SIC and OBS SIC is the smallest, and those values of AMSR-NT2 is almost the worst. It is worth noting that except for SSMIS-NT products which underestimate SIC under all ice conditions corresponding to OBS data, the other five PM products tend to underestimate SIC under light ice condition (OBS SIC = 0 to 30%) and overestimate SIC under other ice conditions (OBS SIC = 30% to 100%). Overall, these five PM products tend to overestimate SIC. In summary, SSMIS-NT, AMSR-BT and AMSR-ASI PM products have better accuracy in SIC retrievals in the summer Arctic. However, AMSR-BT product and AMSR-ASI product based on AMSR sensors have greater advantages for navigation and small-scale marine engineering applications because of their higher spatial resolution.

To our knowledge, in the Arctic, there is no comparison between the OBS SIC and PM SIC with such a large quantity and such a large time span. Therefore, we firmly believe that the results of our comparisons are reliable. The results of this paper will help us understand the limitations of each PM SIC algorithm better, and provide some data references for improving these PM SIC algorithms.

***Acknowledgements***

We Thank all the previous Chinese national Arctic research expeditioners for their supports and

their hard and meticulous works. We Thank the NSIDC and University of Bremen for providing the PM SIC products.

**References**

Andersen S, Tonboe R, Kaleschke L, et al. 2007. Intercomparison of passive microwave sea ice concentration retrievals over the high-concentration Arctic sea ice. Journal of Geophysical Research-Oceans, 112(C8): C08004, doi: 10.1029/2006JC003543

Beitsch A, Kaleschke L, Kern S. 2014. Investigating high-resolution AMSR2 sea ice concentrations during the February 2013 fracture event in the Beaufort Sea. Remote Sensing, 6(5): 3841-3856, doi: 10.3390/rs6053841

Beitsch A, Kern S, Kaleschke L. 2015. Comparison of SSM/I and AMSR-E sea ice concentrations with ASPeCt ship observations around Antarctica. IEEE Transactions on Geoscience and Remote Sensing, 53(4): 1985-1996, doi: 10.1109/TGRS.2014.2351497

Chen Ping, Zhao Jinping. 2017. Variation of sea ice extent in different regions of the Arctic Ocean. Acta Oceanologica Sinica, 36(8): 9-19, doi: 10.1007/s13131-016-0886-x

Cohen J, Screen J A, Furtado J C, et al. 2014. Recent Arctic amplification and extreme mid-latitude weather. Nature Geoscience, 7(9): 627-637, doi: 10.1038/NGEO2234

Comiso J C, Cavalieri D J, Parkinson C L, et al. 1997. Passive microwave algorithms for sea ice concentration: a comparison of two techniques. Remote Sensing of Environment, 60(3): 357-384, doi: 10.1016/S0034-4257(96)00220-9

Comiso J C. 2002. A rapidly declining perennial sea ice cover in the Arctic. Geophysical Research Letters, 29(20): 1956, doi: 10.1029/2002GL015650

Comiso J C, Nishio F. 2008. Trends in the sea ice cover using enhanced and compatible AMSR-E, SSM/I, and SMMR data. Journal of Geophysical Research-Oceans, 113(C2): C02S07, doi: 10.1029/2007JC004257

Comiso J C. 2012. Large decadal decline of the Arctic multiyear ice cover. Journal of climate, 25(4): 1176-1193, doi: 10.1175/JCLI-D-11-00113.1

Hao Guanghua, Su Jie. 2015. A study of multiyear ice concentration retrieval algorithms using AMSR-E data. Acta Oceanologica Sinica, 34(9): 102-109, doi: 10.1007/s13131-015-0656-1

Hollinger J P, Peirce J L, Poe G A. 1990. SSM/I instrument evaluation. IEEE Transactions on Geoscience and Remote Sensing, 28(5): 781-790, doi: 10.1109/36.58964

Ivanova N, Johannessen O M, Pedersen L T, et al. 2014. Retrieval of arctic sea ice parameters by satellite passive microwave sensors: a comparison of eleven sea ice concentration algorithms. IEEE Transactions on Geoscience and Remote Sensing, 52(11): 7233-7246, doi: 10.1109/TGRS.2014.2310136

Kern S, Heygster G. 2001. Sea-ice concentration retrieval in the Antarctic based on the SSM/I 85.5 GHz polarization. Annals of Glaciology, 33: 109-114, doi: 10.3189/172756401781818905

Kern S, Kaleschke L, Clausi D A, et al. 2003. A comparison of two 85-GHz SSM/I ice concentration algorithms with AVHRR and ERS-2 SAR imagery. IEEE Transactions on Geoscience and Remote Sensing, 41(10): 2294-2306, doi: 10.1109/TGRS.2003.817181

Knuth M A, Ackley S F. 2006. Summer and early-fall sea-ice concentration in the Ross Sea comparison of in situ ASPeCt observations and satellite passive microwave estimates. Annals of Glaciology, 44: 303-309, doi: 10.3189/172756406781811466

Lei Ruibo, Xie Hongjie, Wang Jia, et al. 2015. Changes in sea ice conditions along the Arctic

Northeast Passage from 1979 to 2012. Cold Regions Science and Technology, 119: 132-144, doi: 10.1016/j.coldregions.2015.08.004

Liu Yinghui, Key J R, Frey R A, et al. 2004. Nighttime polar cloud detection with MODIS. Remote Sensing of Environment, 92(2): 181-194, doi: 10.1016/j.rse.2004.06.004

Markus T, Cavalieri D J. 2000. An enhancement of the NASA Team sea ice algorithm. IEEE Transactions on Geoscience and Remote Sensing, 38(3): 1387-1398, doi: 10.1016/j.rse.2004.06.004

McIntire T J, Simpson J J. 2002. Arctic sea ice, cloud, water, and lead classification using neural networks and 1.6-μm data. IEEE Transactions on Geoscience and Remote Sensing, 40(9): 1956-1972, doi: 10.1109/TGRS.2002.803728

Meier W N, Ivanoff A. 2017. Intercalibration of AMSR2 NASA Team 2 algorithm sea ice concentrations with AMSR-E slow rotation data. IEEE Transactions on Geoscience and Remote Sensing, 10(9): 3923-3933, doi: 10.1109/JSTARS.2017.2719624

Overland J, Francis J A, Hall R, et al. 2015. The melting Arctic and midlatitude weather patterns: are they connected? Journal of Climate, 28(20): 7917-7932, doi: 10.1175/JCLI-D-14-00822.1

Ozsoy-Cicek B, Xie H, Ackley S F, et al. 2009. Antarctic summer sea ice concentration and extent: comparison of ODEN 2006 ship observations, satellite passive microwave and NIC sea ice charts. The Cryosphere, 3(1): 1-9, doi: 10.5194/tc-3-1-2009

Ozsoy-Cicek B, Ackley S F, Worby A, et al. 2011. Antarctic sea-ice extents and concentrations: comparison of satellite and ship measurements from International Polar Year cruises. Annals of Glaciology, 52(57): 318-326, doi: 10.3189/172756411795931877

Peng G, Meier W N, Scott D J, et al. 2013. A long-term and reproducible passive microwave sea ice concentration data record for climate studies and monitoring. Earth System Science Data, 5(2): 311-318, doi: 10.5194/essd-5-311-2013

Pithan F, Mauritsen T. 2014. Arctic amplification dominated by temperature feedbacks in contemporary climate models. Nature Geoscience, 7(3): 181-184, doi: 10.1038/NGEO2071

Serreze M C, Meier W N. 2019. The Arctic's sea ice cover: trends, variability, predictability, and comparisons to the Antarctic. Annals of the New York Academy of Sciences, 1436(1): 36-53, doi: 10.1111/nyas.13856

Shi Lijiang, Lu Peng, Cheng Bin, et al. 2015. An assessment of arctic sea ice concentration retrieval based on "HY-2" scanning radiometer data using field observations during CHINARE-2012 and other satellite instruments. Acta Oceanologica Sinica, 34(3): 42-50, doi: 10.1007/s13131-015-0632-9

Shibata H, Izumiyama K, Tateyama K, et al. 2013. Sea-ice coverage variability on the Northern Sea Routes, 1980–2011. Annals of Glaciology, 54(62): 139-148, doi: 10.3189/2013AoG62A123

Smith D M. 1996. Extraction of winter total sea-ice concentration in the Greenland and Barents Seas from SSM/I data. International Journal of Remote Sensing, 17(13): 2625-2646, doi: 10.1080/01431169608949096

Spreen G, Kaleschke L, Heygster G. 2008. Sea ice remote sensing using AMSR-E 89-GHz channels. Journal of Geophysical Research-Oceans, 113(C2): C02S03, doi: 10.1029/2005JC003384

Sui Cuijuan, Zhang Zhanhai, Yu Lejiang, et al. 2017. Sensitivity and nonlinearity of Eurasian winter temperature response to recent Arctic sea ice loss. Acta Oceanologica Sinica, 36(8): 52-58, doi: 10.1007/s13131-017-1018-y

Vihma T. 2014. Effects of Arctic sea ice decline on weather and climate: a review. Surveys in

Geophysics, 35(5): 1175-1214, doi: 10.1007/s10712-014-9284-0

Wang Qingkai, Li Zhijun, Lu Peng, et al. 2018. 2014 summer Arctic sea ice thickness and concentration from shipborne observations. International Journal of Digital Earth, 2018: 1-17, doi: 10.1080/17538947.2017.1421720

Wang Yunhe, Bi Haibo, Huang Haijun, et al. 2019. Satellite-observed trends in the Arctic sea ice concentration for the period 1979–2016. Journal of Oceanology and Limnology, 37(1): 18-37, doi: 10.1007/s00343-019-7284-0

Weissling B, Ackley S, Wagner P, et al. 2009. EISCAM—Digital image acquisition and processing for sea ice parameters from ships. Cold Regions Science and technology, 57(1): 49-60, doi: 10.1016/j.coldregions.2009.01.001

Worby A, Allison I, Dirita V. 1999. A Technique for making ship based observations of Antarctic sea ice thickness and characteristics. Research Report No. 14. Hobart: Australia Antarctic Division

Worby A P, Comiso J C. 2004. Studies of the Antarctic sea ice edge and ice extent from satellite and ship observations. Remote Sensing of Environment, 92(1): 98-111, doi: 10.1016/j.rse.2004.05.007

World Meteorological Organization (WMO). 1970. WMO sea-ice nomenclature: terminology, codes and illustrated glossary. Geneva: Secretariat of the World Meteorological Organization (WMO/OMM/ BMO, No. 259, TP. 145)